New monomers or co-monomers based on the alkoxyfuranone Scaffold: Toward new alternatives to Petroleum-Based structures

Marie Le Dot, Mario Andrés Gomez Fernandez, Anne Langovist, Bruno Charrière, Pierre Gérard, Frédéric Dumur, Norbert Hoffmann, Jacques Lalevée

▶ **To cite this version:**

Marie Le Dot, Mario Andrés Gomez Fernandez, Anne Langovist, Bruno Charrière, Pierre Gérard, et al.. New monomers or co-monomers based on the alkoxyfuranone Scaffold: Toward new alternatives to Petroleum-Based structures. European Polymer Journal, 2024, 215, pp.113259. 10.1016/j.eurpolymj.2024.113259 . hal-04624883

HAL Id: hal-04624883
https://hal.science/hal-04624883

Submitted on 25 Jun 2024

HAL is a multi-disciplinary open access archive for the deposit and dissemination of scientific research documents, whether they are published or not. The documents may come from teaching and research institutions in France or abroad, or from public or private research centers.

L'archive ouverte pluridisciplinaire **HAL**, est destinée au dépôt et à la diffusion de documents scientifiques de niveau recherche, publiés ou non, émanant des établissements d'enseignement et de recherche français ou étrangers, des laboratoires publics ou privés.

New monomers or co-monomers based on the alkoxyfuranone Scaffold: Toward new alternatives to Petroleum-Based structures

Marie Le Dot[1], Mario Andrés Gomez Fernandez[2], Anne Langovist[1], Bruno Charrière[3], Pierre Gérard[3], Frédéric Dumur[4], Norbert Hoffmann[2*], Jacques Lalevée[1*]

[1] Institut de Science des Matériaux de Mulhouse IS2M, UMR CNRS 7361, F-68057 Mulhouse, France
[2] CNRS, Université de Reims Champagne-Ardenne, ICMR, Groupe de Photochimie, UFR Sciences, B.P. 1039, 51687 Reims, France
[3] GRL, Arkema, B.P. 34, 64170 Lacq, France
[4] Aix Marseille Univ., CNRS, ICR, UMR 7273, F-13397 Marseille, France

Abstract: From a circular plastic economy standpoint, environmental issues and more stringent environmental regulations, the search for bio-based monomers possessing innovative structures is an important challenge. Furthermore, several goals must be achieved: 1) the homopolymerization of such bio-based monomers by free radical photopolymerization which require small energy inputs with limited emission of volatile organic compounds (COV) and 2) their copolymerization with Elium® thermoplastic resins to increase biogenic carbon in these novel low-viscosity methacrylic resins developed by Arkema which stands out by combining high mechanical performance and recyclability. The challenge will be, in this context, to maximize the biomass carbon while maintaining or even surpassing the properties exhibited by their petrochemical counterpart. In this work, a series of alkoxyfuranones issued from furfural have been synthetized. Three alkoxyfuranones (AF_1, AF_2, AF_3) varying by the functionality of the side-chain (but-1-ene, acrylate and isopropane) attached–via acetalization of the 5-hydroxy-2(5H)-furanone were studied as potential monomers or co-monomers for free radical polymerization. Homopolymerization of two of them (AF_1 and AF_2) was successfully achieved, but only one leads to a high-Glass Transition temperature (Tg) bio-based polymer. On the other hand, copolymerization with Elium® thermoplastic resins was obtained with different ratio of AF_2 as co-monomer. As a result, the expected gain value such as faster photopolymerization was successfully obtained. Nevertheless, the copolymerization doesn't lead to high Tg polymers.

Keywords: Alkoxyfuranones, bio-based monomers, high-Tg bio-based polymers, copolymerization, Elium® thermoplastic resins

Biomass represents an important feedstock for chemical industry [1].[1] Due to their particular molecular structures, new innovative products become more easily accessible [2].[2] In this context, various monomers have been synthesized. On one hand, conventional monomers as they are also available from fossil resources such as acrylates ~~or ethylene~~ have been prepared from renewable resources [3].[3] On the other hand, new monomers are now daily reported and their polymerization abilities as well as the final polymer properties are studied.

Alkoxyfuranones [4][4] or levoglucosenone [5,6][5,6] are examples of monomers obtained from biomass and possessing novel unusual structures that can be investigated in the context of monomers for polymerization, especially for free radical polymerization. These α,β-unsaturated carbonyl or carboxyl compounds are suitable candidates for radical addition [7,8].[7,8] Biomass derived Alkoxyfuranones are valuable platform compounds, for example for the synthesis of surfactants. We became again interested in these compounds as monomers for free radical polymerization [8,9].[8,9]

A variety of alkoxyfuranones can be easily prepared on a large scale even in research laboratory via photo-oxygenation of furfural **1** [10][10], which is obtained by dehydration of hemicelluloses or pentoses (Scheme 1) [11].[11] Photo-oxygenation involving singlet oxygen can yield 5-hydroxy-2(5*H*)-furanone **2**. Acetalization with alcohols thus furnishes 5-alkoxy-2(5*H*)-furanone **3**. An optimized procedure for the preparation of compound **AF4** on large scale in laboratory has recently been reported in the literature (ref.10 and references cited therein). In a similar way, compound **AF2** can be prepared by acetalization of compound **2** with the acrylate derivative **4**. Compounds **AF1** and **AF3** have been obtained by acetalization with the corresponding alcohols.

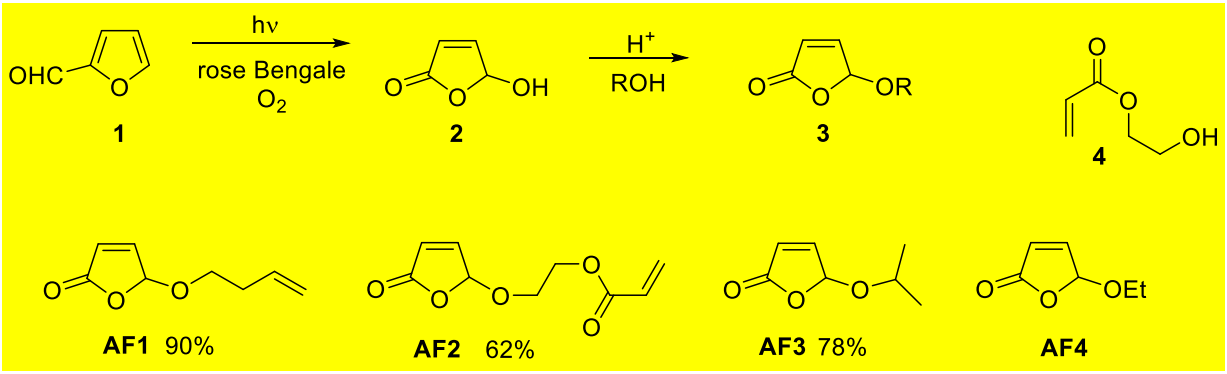

Scheme 1. Synthesis of 5-alkoxy-2(5H)-furanones.

From a material standpoint, commodity plastics such as poly(ethylene terephthalate) (PET), polypropylene (PP), polystyrene (PS), and poly(methyl methacrylate) (PMMA) are mainly produced from fossil fuel-based resources [12,13]. Furthermore, their monomers are often volatile ~~as well as toxic~~ [14, 15]. In this context, biomass derived polymers can be considered as promising candidates to replace petroleum-based polymers due to their potential environmental friendliness, renewability, availability, sustainability. Unfortunately, the (thermo-)mechanical performances of renewable polymers is often inferior compared to traditional petroleum-based polymers [16,17] which limit significantly their implementation to engineering application such as building and public works [18,19], automobile, aeronautics [20], wind energy [21,22], etc.

Thereby, Arkema has developed a novel low-viscosity methacrylic resin called Elium® [23] based on methyl methacrylate (MMA). These resins can be implemented in daily life application as well as in various engineering applications such as composites, medical, optical, nanotechnology, and analytical separations, just to name a few [24]. Elium® resins stand out by combining high mechanical performance and recyclability. Indeed, the potential recycling is quite unique for vinyl polymers considering that the monomer recovery reached up to 90% by chemical recycling [25,26,27]. Nevertheless, poly(meth)acrylates are usually obtained from acrylic and methacrylic acid (AA and MAA) and their corresponding esters using non-sustainable strategies such as propylene oxidation and the Acetone Cyanohydrin Process (ACH) [28,29].

In the present work, the idea was to develop renewable polymers with similar (thermo-)mechanical performances of traditional petroleum-based polymers, with a special focus on their glass transition temperature (Tg). Then, in good agreement with a circular economy approach, the second strategy is to add to Elium® thermoplastic resins high-value co-monomers derived from furfural to increase the ‘‘bio-based content’’ defined as the amount of bio-based carbon in the material or product as a percent of the weight (mass) of the total organic carbon in the product (See Scheme 2) [30]. In this aim, the homopolymerization of the different furanones as well as their copolymerizations with Elium® thermoplastic resins have been investigated.

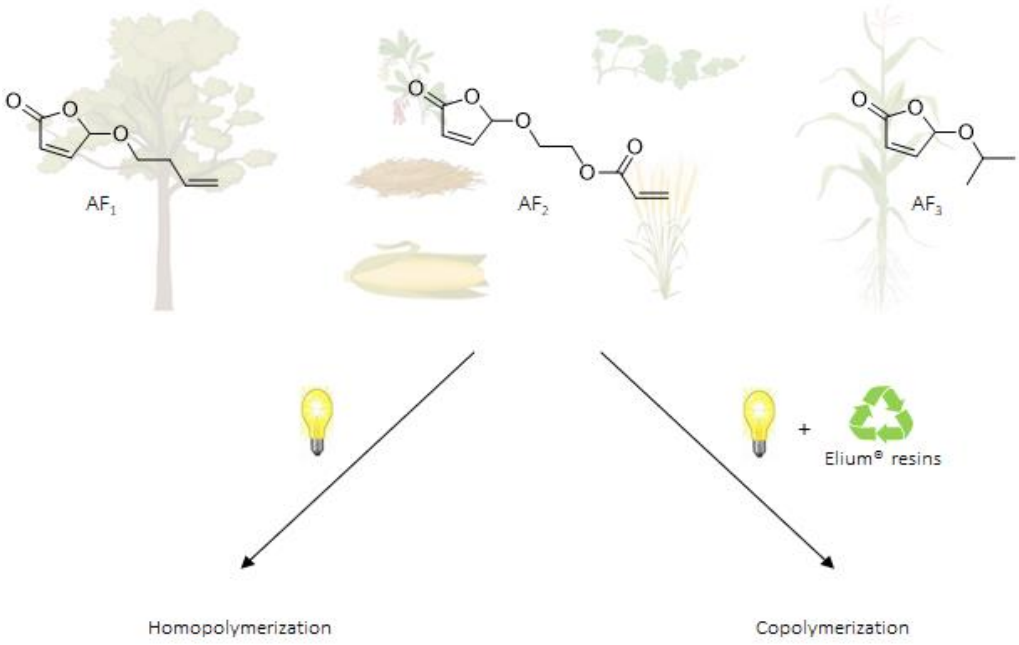

Scheme 2. Two main routes investigated to valorize furfural-derivatives used as potential monomers or co-monomers with Elium® thermoplastic resins in photopolymerization processes

[1] (a) P. Gallezot, *Chem. Soc. Rev.* **2012**, *41*, 1538-1558. (b) C. O. Tuck, E. Pérez, I. Horvath, R. A. Sheldon, M. Poliakoff, *Science* **2012**, *337*, 695-699.
[2] L. T. Mika, E. Cséfalvay, *In Advanced Green Chemistry*, I. T. Horváth, M. Malacria, Eds., World Scientific, pp. 19-76.
[3] T. Pirman, O. Ocepek, B. Likozar, *Ind. Eng. Chem. Res.* **2021**, *60*, 9347-9367.
[4] (a) V. V. Poskonin, D. N. Yakovlev, V. A. Kovardakov, L. A. Badovkaya, *Russ. J. Org. Chem.* **1999**, *35*, 721-726. (b) J. G. H. Hermens, T. Freese, K. J. van den Berg, R. van Gemert, B. L. Feringa, *Sci. Adv.* **2020**, *6*, eabe0026.
[5] (a) Y. Halpern, R. Ritter, A. Broido, *J. Org. Chem.* **1973**, *38*, 204-209. (b) J. He, M. Liu, K. Huang, T. W. Walker, C. T. Maravelias, J. A. Dumesic, G. W. Huber, *Green Chem.* **2017**, *19*, 3642-3653.
[6] S. Fadlallah, A. A. M. Peru, L. Longé, F. Allais, *Polymer Chem.* **2020**, *11*, 7471-7475.
[7] (a) C. Lefebvre, T. Van Gysel, C. Michelin, E. Rousset, D. Djiré, F. Allais, N. Hoffmann, *Eur. J. Org. Chem.* **2022**, *2022*, e202101298. (b) N. Hoffmann, S. Bertrand, S. Marinković, J. Pesch, *Pure Appl. Chem.* **2006**, *78*, 2227-2246. A. G. Griesbeck, N. Hoffmann, K.-D. Warzecha, *Acc. Chem. Res.* **2007**, *40*, 128-140.
[8] A. Gassama, C. Ernenwein, N. Hoffmann, *ChemSusChem* **2009**, *2*, 1130-1137.
[9] X. Yue, Y. Queneau, *ChemSusChem* **2022**, *15*, e202102660.
[10] A. Desvals, M. Fortino, C. Lefebvre, J. Rogier, C. Michelin, S. Alioui, E. Rousset, A. Pedone, G. Lemercier, N. Hoffmann, *New J. Chem.* **2022**, *46*, 8971-8980.
[11] (a) Z. Jiang, D. Hu, Z. Zhao, Z. Yi, Z. Chen, K. Yan, *Processes* **2021**, *9*, 1234. (b) F. Martel, B. Estrine, R. Plantier-Royon, N. Hoffmann, C. Portella, *Top. Curr. Chem.* **2010**, *294*, 79-115.

As shown in Figure 1a, **AF_1** monomer has two potential polymerizable vinyl double bonds as acceptors ($A_{(=)}$: $C=C_1$) or donors ($D_{(=)}$: $C=C_2$), while Elium® resins has only one ($C=C_3$) (the different $C=C_1$, $C=C_2$, $C=C_3$ bonds

are defined in Figure 1a). Different batches of resins were prepared by mixing different weight ratio of Elium® 190 (noted **E** below) with **AF_1**. In each batch was added 3 %wt of BAPO used as photoinitiator. Photopolymerization experiments were carried out during 10 min. under LED irradiation (405 nm; 110 mW/cm^2). The homopolymerization and the copolymerization of **AF_1** with Elium® resins were both studied by FTIR. Deconvolution of the FTIR spectra obtained from different blends of **AF_1** and **E** as well as their corresponding pure monomers lead to establish a structure/property relationship. The carbon-carbon double bond absorption frequency belonging to **E** was identified around 6170 cm^{-1} ($C=C_3$) and the carbon-carbon bond absorption frequencies belonging to the but-1-ene and the furan-2(5*H*)-one of **AF_1** were identified respectively around 6120 cm^{-1} ($C=C_2$) and 6080 cm^{-1} ($C=C_1$), respectively. The degree of conversion obtained from the polymerization of both monomers was achieved by measuring the percentage of carbon-carbon double bonds that have been converted to single bonds to form a polymeric resin. Nevertheless, carbon-carbon absorption bands belonging to both monomers tend to overlaps in a range of 6250 and 6050 cm^{-1} to form a broad and fairly featureless envelope. Thereby, the most successful approach to narrow bands and achieve the desired resolution is via mathematical treatment of the data. Fourier Self-Deconvolution (FSD) and Fourier Band Isolation (FBI) [31] were both used for peak-finding, unravelling multi-component envelopes and obtaining semi-quantitative data (see supporting information, Figure S1). A conversion of nearly 100% of **E** and 56% of **AF_1** (see supporting information, Table S1) were obtained and leads to obtain their respective polymer pellets are shown in Figure 1a. Surprisingly, in presence of **E**, the conversion of **AF_1** appeared as being inhibited and does not any longer lead to obtain polymers pellets for high amount of **AF_1** (over 25 %wt). Indeed, the peak area of $C=C_1$ and $C=C_2$ before (Figure 1b) and after irradiation (Figure 1c) remains nearly similar, unlike $C=C_3$ which fully disappeared**.** To sum up, homopolymerization was achieved for **AF_1** monomers. Nevertheless, the copolymerization with Elium® resins of this first bio-based monomer does not look to occur. Thereby, the expected gain value such as a faster photopolymerization, a high Tg for the resulting polymer wasn't achieved by adding **AF_1** in Elium® thermoplastic resins.

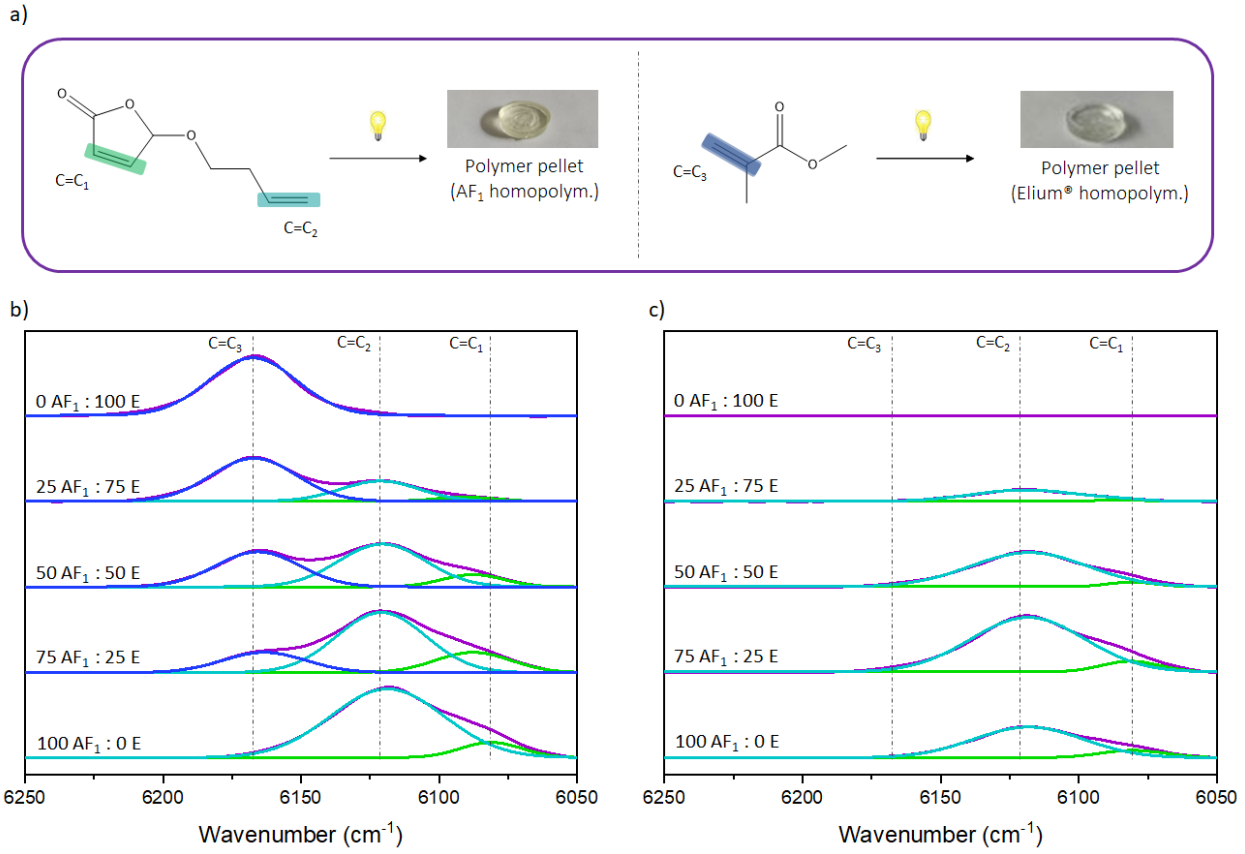

Figure 1. a) Proposed property-structure correlation between monomers and the RT-FTIR spectra obtained and polymer pellets obtained after the homopolymerization of ***AF₁*** *and Elium® resins. RT-FTIR spectra obtained from Elium® 190 (E) mixed with different weight ratios of* ***AF₁*** *fitted to three C=C bonds centred at around 6170 cm^{-1} (C=C$_3$), 6120 cm^{-1} (C=C$_2$) and 6080 cm^{-1} (C=C$_1$) b) before polymerization and c) after polymerization.*

In Table 1 are summarized the final function conversions of both monomers as well as the aspect and the Tg associated to their polymer pellets. The drop of conversions of **AF₁** is in well coherence with the liquid aspects obtained with higher amount of **AF₁** in presence of **E**. If the polymerization of **AF₁** is inhibited, the polymerization of Elium® resin remains fully complete with a conversion of 100% independently of the amount of **AF₁** add to the blends. Nevertheless, the homopolymerization of **AF₁** monomer leads to high-Tg bio-based polymers. The associated Tg was determined around 142°C.

Formulations	AF_1 Conversion (%)	Elium® 190 Conversion (%)	Aspect	Tg (°C)
0 AF_1 : 100 E		100	Solid *(Elium® homopolym.)*	89
25 AF_1 : 75 E	28	100	Solid *(Elium® homopolym.)*	31
50 AF_1 : 50 E	6	100	Gel *(Elium® homopolym.)*	Not determined
75 AF_1 : 25 E	1	100	Liquid *(Elium® homopolym.)*	Not determined
100 AF_1 : 0 E	56		Solid *(AF_1 homopolym.)*	142

*Table 1: Intrinsic conversions obtained from Elium® 190 (**E**) and **AF_1** monomers in different blend ratios, as well as the aspects and Tg obtained from the corresponding polymer pellets.*

In order to increase the bio-based content in Elium® resins, an alkoxyfuranone with an acrylate end group (**AF_2**) was synthetized to copolymerize with **E**. Once again, different batches of resins were prepared by mixing different weight ratios of **E** with **AF_2**. Homopolymerization and copolymerization were both successfully achieved with high conversions of both monomers. Once again, deconvolution of the FTIR spectra obtained from the formulations containing different weight ratios of **AF_2** and **E** as well as their corresponding pure monomers lead to establish a structure performance relationship (Figure 2a). The carbon-carbon bond absorption frequency belonging to Elium® resin and acrylate end group of **AF_2** were both identified around 6170 cm^{-1} ($C=C_{2\ or/and\ 3}$) and the carbon-carbon double bond absorption frequencies belonging to the furan-2(5*H*)-one of **AF_2** were identified around 6128 cm^{-1} ($C=C_1$), 6107 cm^{-1} ($C=C_1$) and 6084 cm^{-1} ($C=C_1$). Identification of the different C=C bonds is given in Figure 2a. Homopolymerization of Elium® resin as well as **AF_2** were monitored by RT-FTIR. Conversions of nearly 100% and 96% (see supporting information, Table S1) were obtained respectively and led to obtain high conversion polymer pellets as shown in Figure 2a. In the presence of Elium® resin, the conversion of **AF_2** remained nearly 100% and thereby led to obtained fully cured polymers. Indeed, all the peak areas in presence of Elium® resins before (Figure 2b) and after irradiation (Figure 2c) fully disappeared (see supporting information, Table S2). To sum up, homopolymerization and copolymerization were both successfully achieved for **AF_2** monomers.

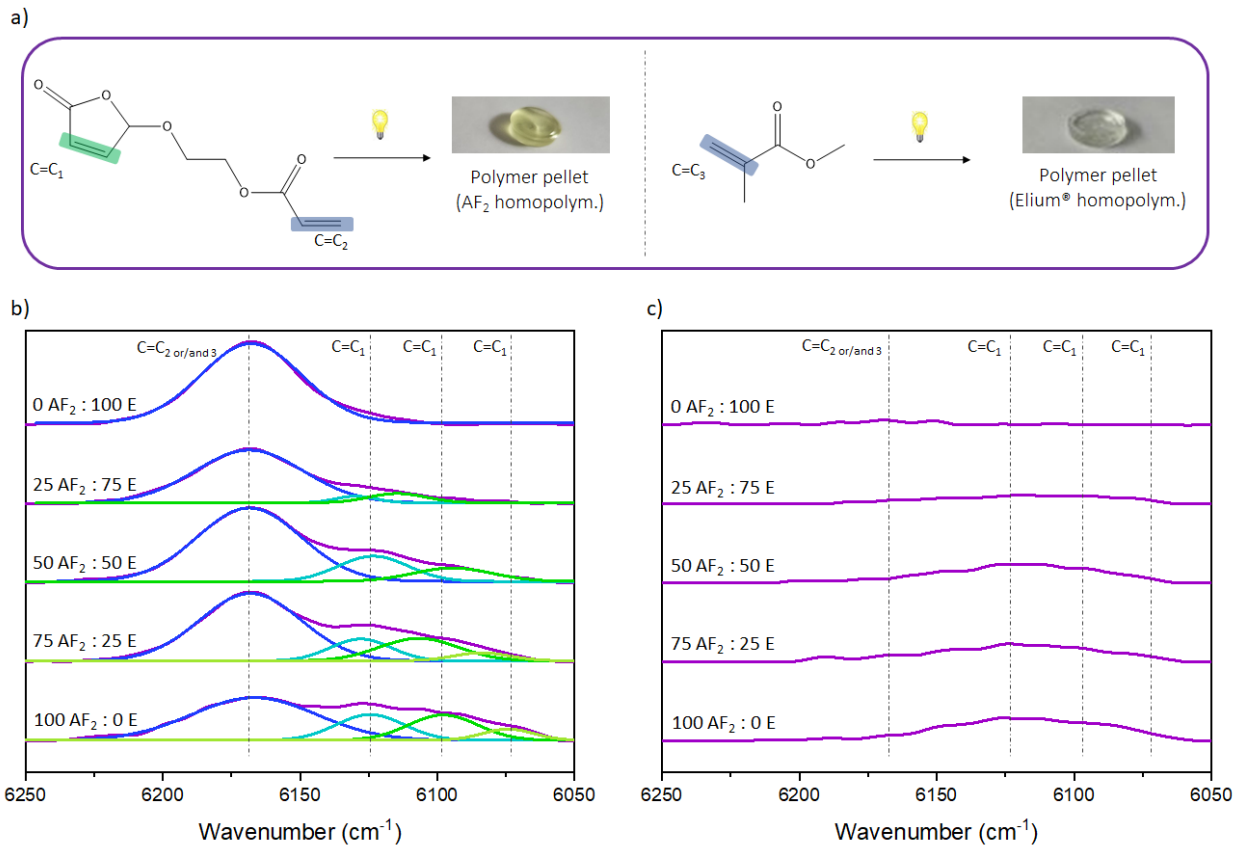

*Figure 2: a) Proposed property-structure correlation between monomers and the RT-FTIR spectra obtained and polymer pellets obtained after the homopolymerization of **AF_2** and Elium® resins. RT-FTIR spectra obtained from **E** mixed with different weight ratios of **AF_2** fitted to four C=C bond peaks centred at around 6170 cm^{-1} ($C=C_{2\ or\ and\ 3}$), 6128 cm^{-1} ($C=C_1$), 6107 cm^{-1} ($C=C_1$) and 6084 cm^{-1} ($C=C_1$) b) before polymerization and c) after polymerization.*

In Figure 3, a special focus on the advantages and disadvantages of using **AF_2** as a monomer or a co-monomer with Elium® thermoplastic resin was investigated in detail. In Figure 3b, kinetic of polymerization was monitored by RT-FTIR. Higher polymerization rates were observed for **AF_2** (curve 5) compared to the polymerization of **E** (curve 1). Thereby, polymerization kinetics obtained from the copolymerization of **AF_2** with **E** are faster when the amount of **AF_2** increases (see curves 2, 3, 4). In Figure 3c, thermograms obtained from the resulting polymers pellets are compared. The Tg obtained from **AF_2** (curve 5) is much lower compared to the one obtained from Elium® polymer pellet (curve 1). Consequently, the Tg obtained from the copolymerization of **AF_2** with **E** decreases when the amount of **AF_2** increases (see curve 2, 3, 4). To sum up, by using **AF_2** as a co-monomer allowed a faster polymerization of **E** and the thermograms obtained from the copolymers pellets highlight a drop of the thermo-mechanical properties of the final polymers.

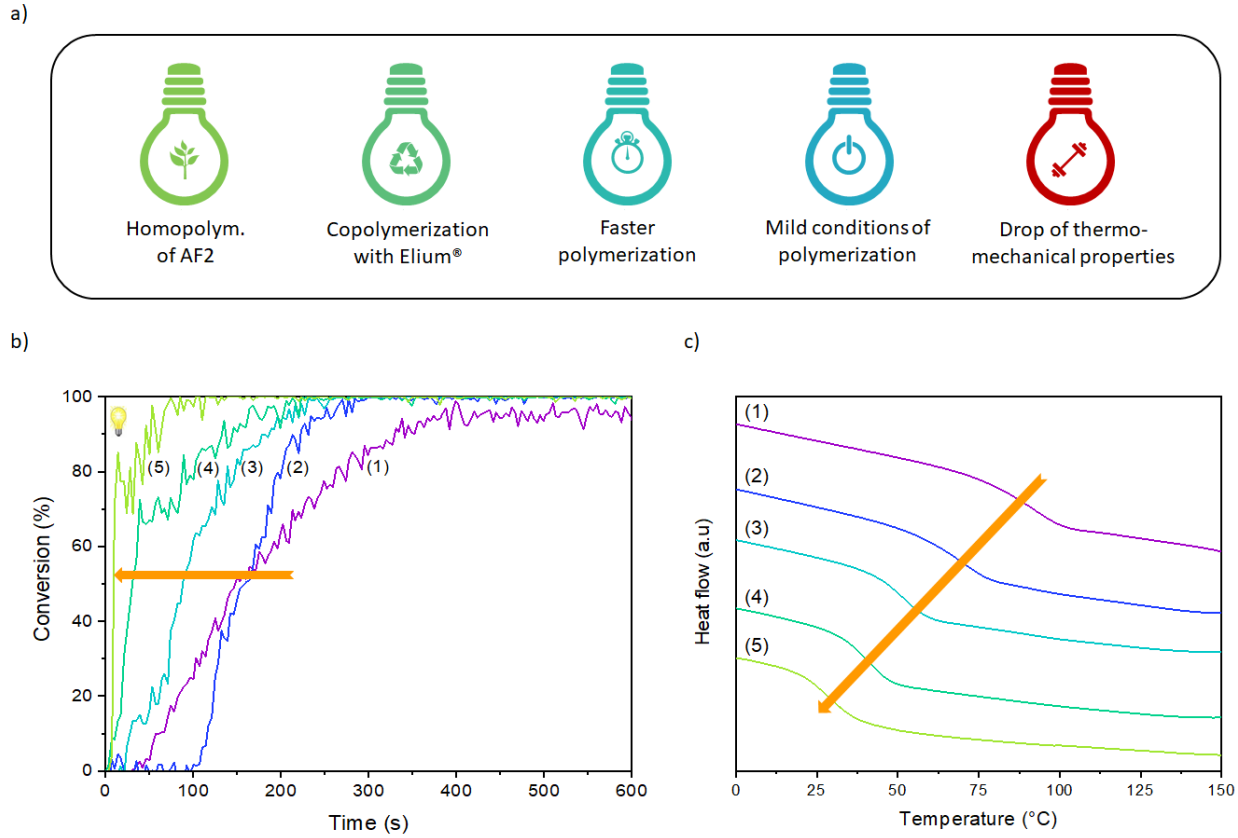

Figure 3: a) Summarized advantages and disadvantages of ***AF_2*** *polymerization with* ***E****; b) RT-FTIR polymerization kinetics of XX functions during the homopolymerization of* ***AF_2*** *(curve 5) and Elium® resins (curve 1) as well as the copolymerization using different weigh ratio of* ***AF_2/E*** *: 25%* ***AF_2*** *: 75%* ***E*** *(w/w; curve 2), 50%* ***AF_2*** *: 50%* ***E*** *(w/w; curve 3) and 75%* ***AF_2*** *: 25%* ***E*** *(w/w; curve 4); c) DSC thermograms of corresponding polymers obtained after polymerization under mild condition (LED 405 nm; 110 mW/cm²).*

In Table 2 are summarized the final conversions of both monomers as well as the aspect and the Tg associated to the polymers. If the conversion of both monomers is nearly 100%, the drop of Tg of the materials obtained from the different blends constitute a significant drawback to the implementation of this bio-based Elium® resins obtained from its copolymerization with **AF_2**. The intrinsic Tg of **AF_2** was established around 29°C, and the Tg of the copolymers issued from Elium® resins and **AF_2** blends decreases when the amount of furanone increases.

Formulations	Curing/Gel Time (s)	AF_2 Conversion (%)	Elium® 190 Conversion (%)	Aspect	Tg (°C)
0 AF_2 : 100 E	388		100	Solid *(Elium® homopolym.)*	89
25 AF_2 : 75 E	285	100	100	Solid *(copolymerization)*	69
50 AF_2 : 50 E	231	100	100	Solid *(copolymerization)*	52
75 AF_2 : 25 E	167	100	100	Solid *(copolymerization)*	41
100 AF_2 : 0 E	72	96		Solid *(AF_2 homopolym.)*	29

*Table 2: Intrinsic conversion obtained from Elium® 190 (**E**) and **AF_2** monomers in different blend ratios, as well as the aspects and Tg obtained from the corresponding polymers.*

Unfortunately, the homopolymerization and the copolymerization of **AF_3** weren't achieved and doesn't lead to any polymeric materials (see supporting information, Figure S3). This was expected due to the low ability of furanone to homopolymerize.

Conclusion: In this study, three original alkoxyfuranones (**AF_1**, **AF_2** and **AF_3**) were synthetized to obtain high-Tg bio-based monomers or bio-based co-monomers compatible with the chemistry of Elium® thermoplastic resins. Photopolymerization was carried out to combined high efficient energy process and materials, which are more environmentally sustainable. Property-structure correlation as well as Fourier Self-Deconvolution (FSD) and Fourier Band Isolation (FBI) have led to establish the homopolymerization of **AF1** and **AF2** and the co-polymerization of **AF_2** with Elium® thermoplastic resins. The glass-transition temperature of the polymeric materials resulting from the homopolymerization of **AF_2** is relatively low (Tg = 29°C) in contrast to the one obtained from **AF_1** (Tg established around 142°C). Thereby, the high thermo-mechanical properties of this material could be highly suitable for a wide range of applications. From the copolymerization point of view, adding **AF_2** to Elium® resins allowed a faster polymerization process compared to pure Elium®. Unfortunately, a drop of Tg was also evidenced, thus constraining the implementation of **AF2** and Elium® blends. Other biosourced monomers compatible with Elium resin will be studied in forthcoming works.

References:

[1]: (a) P. Gallezot, *Chem. Soc. Rev.* **2012**, *41*, 1538-1558. (b) C. O. Tuck, E. Pérez, I. Horvath, R. A. Sheldon, M. Poliakoff, *Science* **2012**, *337*, 695-699.

[2]: L. T. Mika, E. Cséfalvay, *In Advanced Green Chemistry*, I. T. Horváth, M. Malacria, Eds., World Scientific, pp. 19-76.

[3]: T. Pirman, O. Ocepek, B. Likozar, *Ind. Eng. Chem. Res.* **2021**, *60*, 9347-9367.

[4]: (a) V. V. Poskonin, D. N. Yakovlev, V. A. Kovardakov, L. A. Badovkaya, *Russ. J. Org. Chem.* **1999**, *35*, 721-726. (b) J. G. H. Hermens, T. Freese, K. J. van den Berg, R. van Gemert, B. L. Feringa, *Sci. Adv.* **2020**, *6*, eabe0026.

[5]: (a) Y. Halpern, R. Ritter, A. Broido, *J. Org. Chem.* **1973**, *38*, 204-209. (b) J. He, M. Liu, K. Huang, T. W. Walker, C. T. Maravelias, J. A. Dumesic, G. W. Huber, *Green Chem.* **2017**, *19*, 3642-3653.

[6]: S. Fadlallah, A. A. M. Peru, L. Longé, F. Allais, *Polymer Chem.* **2020**, *11*, 7471-7475.

[7]: (a) C. Lefebvre, T. Van Gysel, C. Michelin, E. Rousset, D. Djiré, F. Allais, N. Hoffmann, *Eur. J. Org. Chem.* **2022**, *2022*, e202101298. (b) N. Hoffmann, S. Bertrand, S. Marinković, J. Pesch, *Pure Appl. Chem.* **2006**, *78*, 2227-2246. A. G. Griesbeck, N. Hoffmann, K.-D. Warzecha, *Acc. Chem. Res.* **2007**, *40*, 128-140.

[8]: A. Gassama, C. Ernenwein, N. Hoffmann, *ChemSusChem* **2009**, *2*, 1130-1137.

[9]: X. Yue, Y. Queneau, *ChemSusChem* **2022**, *15*, e202102660.

[10]: A. Desvals, M. Fortino, C. Lefebvre, J. Rogier, C. Michelin, S. Alioui, E. Rousset, A. Pedone, G. Lemercier, N. Hoffmann, *New J. Chem.* **2022**, *46*, 8971-8980.

[11]: (a) Z. Jiang, D. Hu, Z. Zhao, Z. Yi, Z. Chen, K. Yan, *Processes* **2021**, *9*, 1234. (b) F. Martel, B. Estrine, R. Plantier-Royon, N. Hoffmann, C. Portella, *Top. Curr. Chem.* **2010**, *294*, 79-115.

[12] : NAGALAKSHMAIAH, Malladi, AFRIN, Sadaf, MALLADI, Rajini Priya, *et al.* Biocomposites: Present trends and challenges for the future. *Green composites for automotive applications*, 2019, p. 197-215.

[13]: VEITH, Clémence, DIOT-NÉANT, Florian, MILLER, Stephen A., *et al.* Synthesis and polymerization of bio-based acrylates: A review. *Polymer Chemistry*, 2020, vol. 11, no 47, p. 7452-7470.

[14]: HUFF, James et INFANTE, Peter F. Styrene exposure and risk of cancer. *Mutagenesis*, 2011, vol. 26, no 5, p. 583-584.

[15]: CALAFAT, Antonia M., YE, Xiaoyun, WONG, Lee-Yang, *et al.* Exposure of the US population to bisphenol A and 4-tertiary-octylphenol: 2003–2004. *Environmental health perspectives*, 2008, vol. 116, no 1, p. 39-44.

[16]: MOHIUDDIN, M., KUMAR, B., et HAQUE, SJBCIE. Biopolymer composites in photovoltaics and photodetectors. *Biopolymer composites in electronics*, 2017, p. 459-486.

[17]: LEE, Koon-Yang et BISMARCK, Alexander. Bacterial nanocellulose as reinforcement for polymer matrices. In : *Bacterial Nanocellulose*. Elsevier, 2016. p. 109-122.

[18]: BENMOKRANE, Brahim, CHAALLAL, Omar, and MASMOUDI, Radhouane. Glass fibre reinforced plastic (GFRP) rebars for concrete structures. *Construction and Building Materials*, 1995, vol. 9, no 6, p. 353-364.

[19]: HENSHER, David A. *Fiber-reinforced-plastic (FRP) reinforcement for concrete structures: properties and applications*. Elsevier, 2016.

[20]: ARIF, Mohammad, ASIF, Mohammad, and AHMED, Israr. Advanced composite material for aerospace application—A review. *Int. J. Eng. Manuf. Sci*, 2017, vol. 7, no 2, p. 393-409

[21]: *JURECZKO*, M., PAWLAK, M. and MEZYK, A. Optimisation of wind turbine blades. *Journal of materials processing technology*, 2005, vol. 167, no 2-3, p. 463-471.

[22]: LEFEUVRE, Anaële, GARNIER, Sébastien, JACQUEMIN, Leslie, *and al.* Anticipating in-use stocks of carbon fibre reinforced polymers and related waste generated by the wind power sector until 2050. *Resources, Conservation and Recycling*, 2019, vol. 141, p. 30-39.

[23]: KAZEMI, M. E., SHANMUGAM, Logesh, LU, Dong, *and al.* Mechanical properties and failure modes of hybrid fiber reinforced polymer composites with a novel liquid thermoplastic resin, Elium®. *Composites Part A: Applied Science and Manufacturing*, 2019, vol. 125, p. 105523.

[24]: ALI, Umar, KARIM, Khairil Juhanni Bt Abd, et BUANG, Nor Aziah. A review of the properties and applications of poly (methyl methacrylate)(PMMA). *Polymer Reviews*, 2015, vol. 55, no 4, p. 678-705.

[25]: MOENS, Eli KC, DE SMIT, Kyann, MARIEN, Yoshi W., *and al.* Progress in reaction mechanisms and reactor technologies for thermochemical recycling of poly (methyl methacrylate). *Polymers*, 2020, vol. 12, no 8, p. 1667.

[26] : DE TOMMASO, Jacopo and DUBOIS, Jean-Luc. Risk Analysis on PMMA Recycling Economics. *Polymers*, 2021, vol. 13, no 16, p. 2724.

[27]: DE SMIT, Kyann, MARIEN, Yoshi W., VAN GEEM, Kevin M., *and al.* Connecting polymer synthesis and chemical recycling on a chain-by-chain basis: a unified matrix-based kinetic Monte Carlo strategy. *Reaction Chemistry & Engineering*, 2020, vol. 5, no 10, p. 1909-1928.

[28]: NAGAI, Koichi. New developments in the production of methyl methacrylate. *Applied Catalysis A: General*, 2001, vol. 221, no 1-2, p. 367-377.

[29]: PORCELLI, R. V. et JURAN, B. Selecting the process for your next MMA plant. *Hydrocarbon Process.;(United States)*, 1986, vol. 65, no 3.

[30]: NARAYAN, Ramani. Carbon footprint of bioplastics using biocarbon content analysis and life-cycle assessment. *MRS bulletin*, 2011, vol. 36, no 9, p. 716-721.

[31]: TOOKE, P. B. Fourier self-deconvolution in IR spectroscopy. *TrAC Trends in Analytical Chemistry*, 1988, vol. 7, no 4, p. 130-136.

Supporting information

New Bio-based Monomers or Co-monomers Based on the Furfural Scaffold: Toward New Alternatives to Petrosourced -Based Structures

Marie Le Dot[1], Mario Andrés Gomez Fernandez[2], Pierre Gerard[3], Frédéric Dumur[4], Norbert Hoffmann[2*], Jacques Lalevée[1*]

[1] Institut de Science des Matériaux de Mulhouse IS2M, UMR CNRS 7361, F-68057 Mulhouse, France
[2] CNRS, Université de Reims Champagne-Ardenne, ICMR, Groupe de Photochimie, UFR Sciences, B.P. 1039, 51687 Reims, France
[3] GRL, Arkema, B.P. 34, 64170 Lacq, France
[4] Aix Marseille Univ., CNRS, ICR, UMR 7273, F-13397 Marseille, France

Experimental part

General. All commercially available compounds and solvents were purchased from Aldrich Chemical Co., Alfa Aesar, ABCR or TCI and used as received. All reactions were performed under air atmosphere unless otherwise specified

Analytical thin layer chromatography (TLC) was performed on pre-coated TLC sheets Alugram Xtrasil G/UV 250 Macherey-Negel, visualized either with a UV lamp (254 nm) or by using the appropriate solution of stain followed by heating. Flash column chromatography was performed on silica gel (230-400 mesh).

^{1}H NMR and ^{13}C NMR spectra were recorded on a Bruker 500 MHz spectrometer in $CDCl_3$ (unless otherwise specified). The observed signals are reported as follows: chemical shift in parts per million from tetramethylsilane. Spectra were calibrated to the respective residual solvent signals for $CDCl_3$ [δ (^{1}H)=7.26 ppm, δ (^{13}C) = 77.16 ppm], for CD_3CN [δ (^{1}H)=1.94 ppm, δ (^{13}C) = 118.26 ppm]. The following abbreviations for single multiplicities were used: br-broad, s-singlet, d-doublet, t-triplet, q-quartet, quint-quintuplet, sext-sextet, m-multiplet or overlap of non-equivalent resonances. Apparent multiplets which occur as a result of coupling constant equality between magnetically non-equivalent protons are marked as virtual (virt.).

Coupling constants (*J*) are reported in Hertz (Hz). All NMR spectra were obtained at rt unless otherwise specified.

High-resolution mass spectrometry (HR-MS) data were recorded using a spectrometer equipped with an electrospray ionisation source (ESI), in positive mode associated with a TOF analyzer.

2-((5-oxo-2,5-dihydrofuran-2-yl)oxy)ethyl acrylate

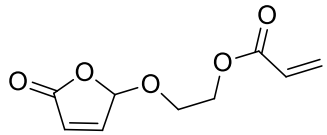

Chemical Formula: $C_9H_{10}O_5$
Exact Mass: 198,05

2-((5-Oxo-2,5-dihydrofuran-2-yl)oxy)ethyl acrylate was obtained from 5-hydroxyfuran-2(5*H*)-one (5.13 g, 51.29 mmol) using 2-hydroxyethyl acrylate (6.29 g, 54.17 mmol) in the presence of APTS (0.165 g, 0.95 mmol) and the mixture was heated to reflux in 50 mL of $CHCl_3$ for 4 hours using the inversed Dean-Stark apparatus. After cooling, the solvent ($CHCl_3$) was evaporated under reduced pressure and the reaction mixture dissolved in CH_2Cl_2 (150 mL), washed 1x with aqueous NaOH (3M, 200 mL) and then with brine, dried using $MgSO_4$, filtrated and evaporated to obtain the crude. After purification, a transparent oil was obtained containing 2-((5-oxo-2,5-dihydrofuran-2-yl)oxy)ethyl acrylate (6.25 g, 62% yield).

TLC: R_f = 0.1 (Petroleum ether/EtOAc, 9:1) [$KMnO_4$].
^{1}H NMR (500 MHz, $CDCl_3$) δ 3.97 (ddd, *J* = 11.2, 6.6, 3.2 Hz, 1H), 4.10 (ddd, *J* = 11.2, 5.9, 3.1 Hz, 1H), 4.35 (ddd, *J* = 12.4, 6.6, 3.1 Hz, 1H), 4.43 (ddd, *J* = 12.4, 5.9, 3.2 Hz, 1H), 5.89 (dd, *J* = 10.5, 1.3 Hz, 1H), 6.00 (t, *J* = 1.1 Hz, 1H), 6.17 (dd. *J* = 17.3, 10.5 Hz, 1H), 6.27 (dd, *J* = 5.7, .1.1 Hz, 1H), 6.46 (dd, *J* = 17.3, 1.2 Hz, 1H), 7.25 (dd, *J* = 5.7, 1.2 Hz, 1H).

^{13}C NMR (125 MHz, $CDCl_3$) δ 62.91, 67.81, 102.91, 125.31, 127.96, 131.50, 150.00, 165.95, 170.16.

HRMS (ESI) m/z: $[C_9H_{10}O_5+Na]^+$ Calculated: 221.0426; found 221.0424.

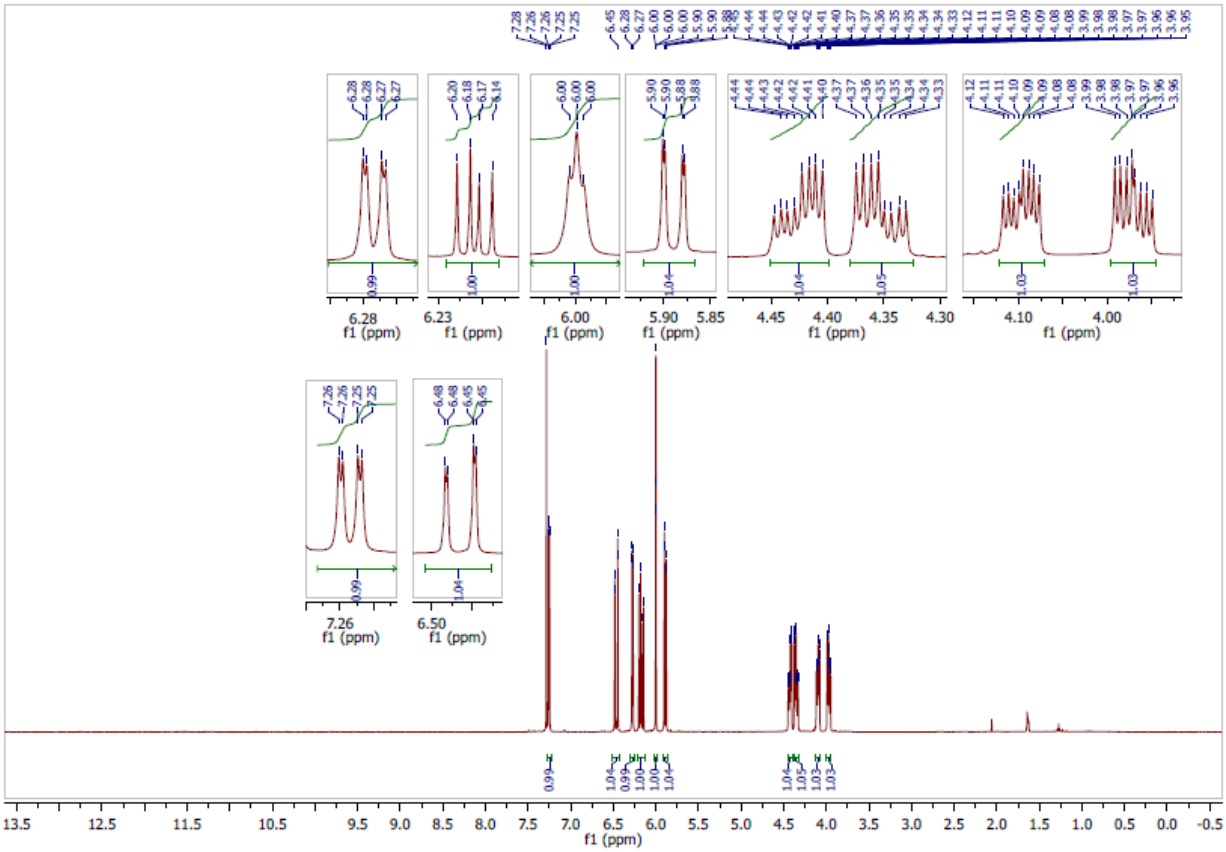
f1 (ppm)

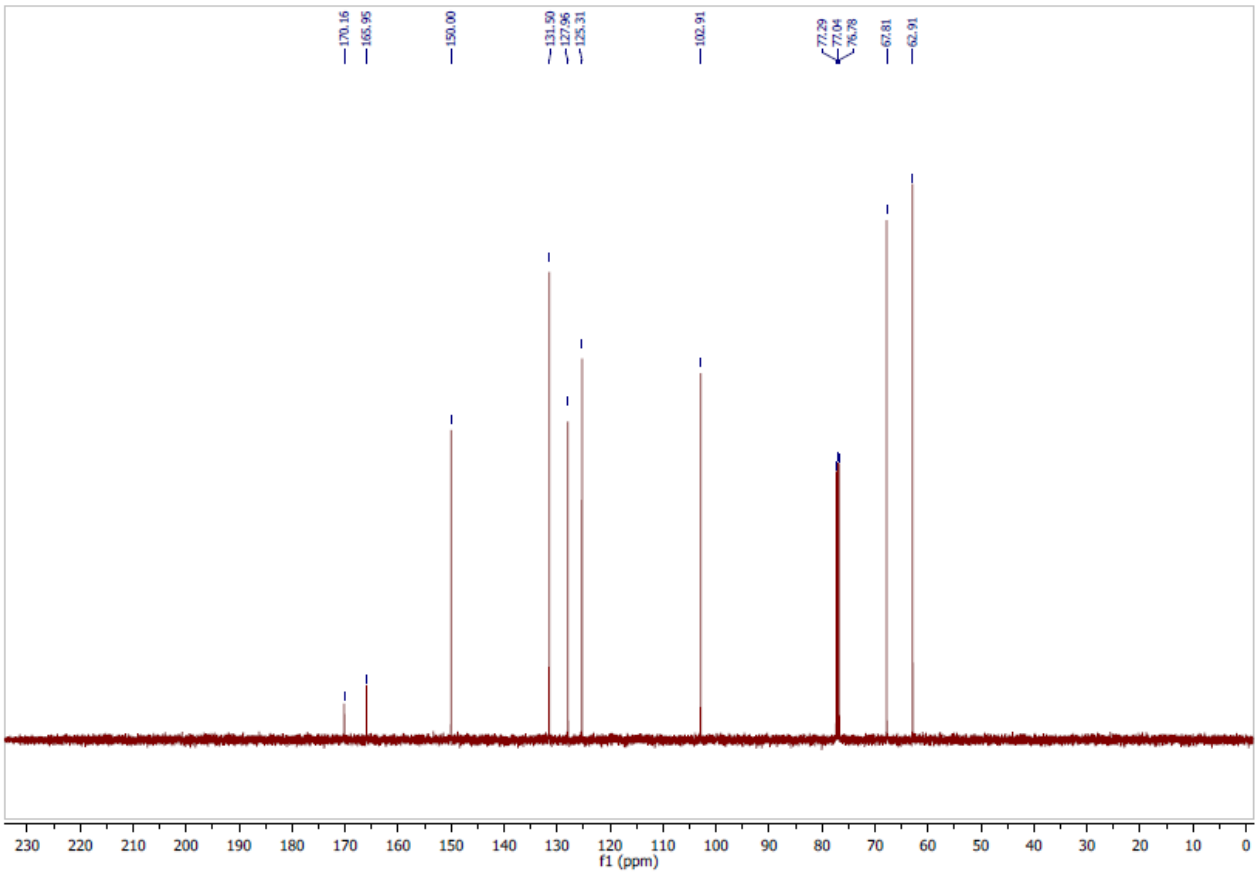
170.16
165.95
150.00
131.50
127.96
125.31
102.91
77.29
77.04
76.78
67.81
62.91
230 220 210 200 190 180 170 160 150 140 130 120 110 100 90 80 70 60 50 40 30 20 10 0
f1 (ppm)

5-isopropoxyfuran-2(5H)-one

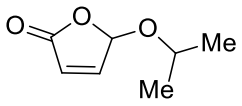

Chemical Formula: $C_7H_{10}O_3$
Exact Mass: 142,06

5-Isopropoxyfuran-2(5*H*)-one was obtained from 5-hydroxyfuran-2(5*H*)-one (3.07 g, 30.69 mmol) using propan-2-ol (2.45 g, 40.75 mmol) in the presence of APTS (0.210 g, 1.21 mmol). After purification, a transparent oil was obtained containing 5-isopropoxyfuran-2(5*H*)-one 3.42 g, 78% yield. The ^{1}H NMR spectrum is in agreement with the previously data reported by Feringa et al.[12]

TLC: R_f = 0.5 (Petroleum ether/EtOAc, 6:4) [$KMnO_4$].

^{1}H NMR (500 MHz, $CDCl_3$) δ 1.26 (d, *J* = 6.2 Hz, 3H), 1.29 (d, *J* = 6.3 Hz, 3H), 4.06-4.09 (m, 1H), 6.00 (s, 1H), 6.20 (d, *J* = 5.6 Hz, 1H), 7.17 (d, *J* = 5.6 Hz, 1H).

^{13}C NMR (125 MHz, $CDCl_3$) δ 22.09, 23.29, 73.83, 102.24, 124.92, 150.84, 170.87.

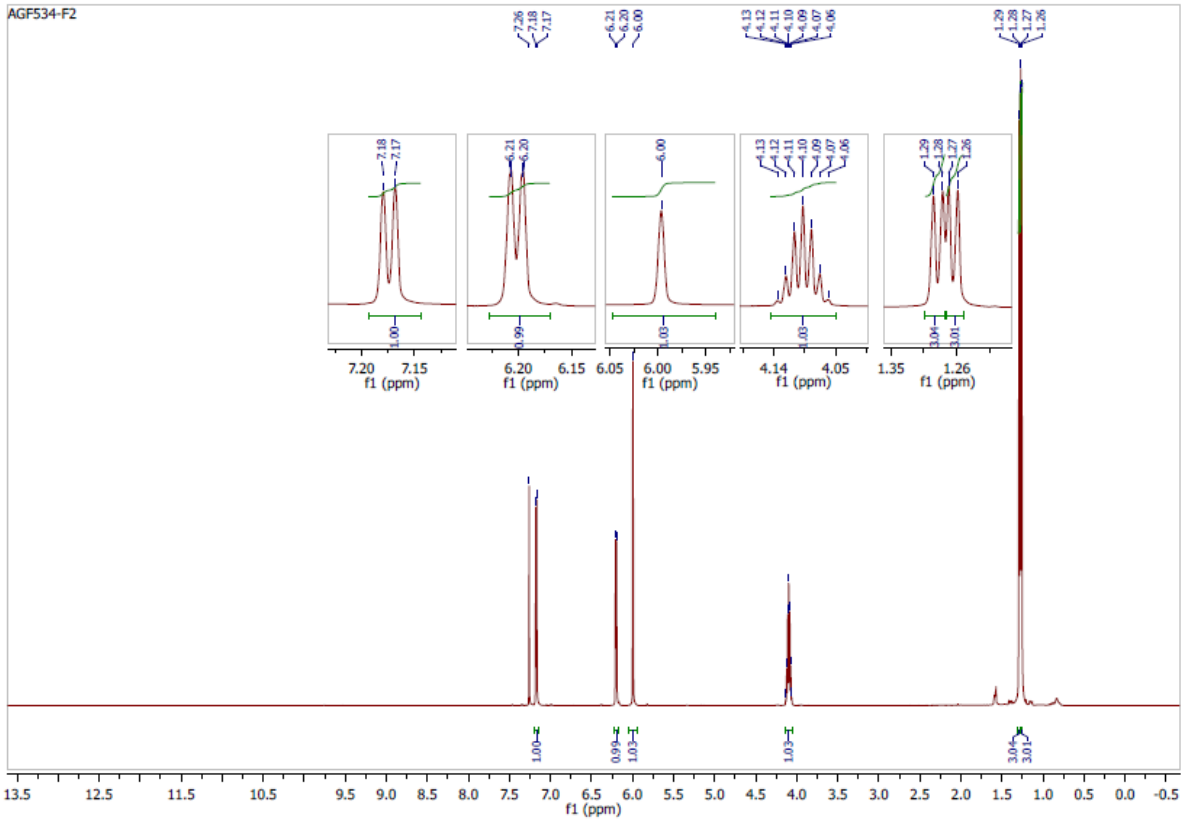

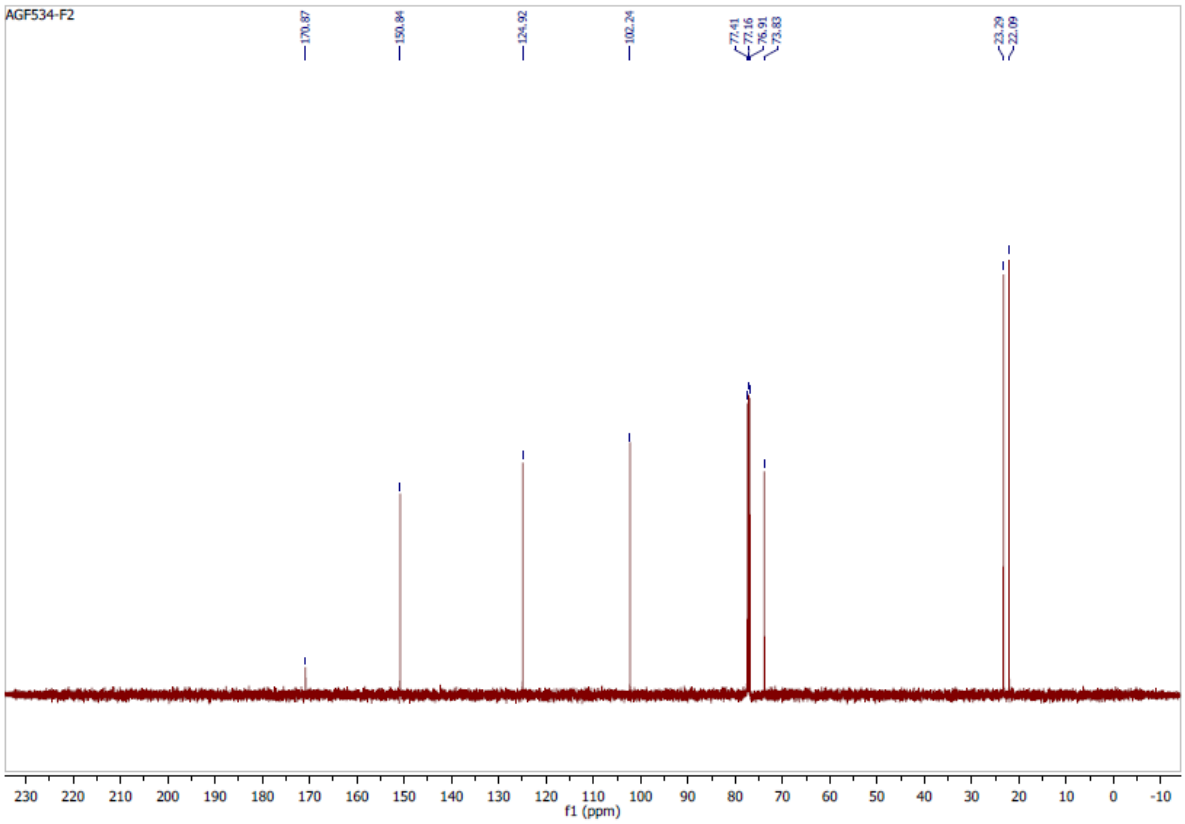
AGF534-F2
170.87
150.84
124.92
102.24
77.41
77.16
76.91
73.83
23.29
22.09
230 220 210 200 190 180 170 160 150 140 130 120 110 100 90 80 70 60 50 40 30 20 10 0 -10
f1 (ppm)

5-(but-3-en-1-yloxy)furan-2(5H)-one

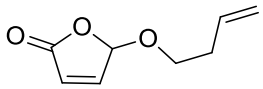

Chemical Formula: $C_8H_{10}O_3$
Exact Mass: 154,06

5-(But-3-en-1-yloxy)furan-2(5*H*)-one was obtained from 5-hydroxyfuran-2(5*H*)-one (5.04 g, 50.35 mmol) using 3-buten-1-ol (4.01 g, 55.60 mmol) in the presence of APTS (0.128 g, 0.74 mmol). After purification, a transparent oil was obtained containing 5-(but-3-en-1-yloxy)furan-2(5*H*)-one (7.01 g, 90% yield).

TLC: R_f = 0.23 (Petroleum ether/EtOAc, 9:1) [$KMnO_4$].

^{1}H NMR (500 MHz, $CDCl_3$) δ 2.36-2.43 (m, 2H), 3.70-3.76 (m, 1H), 3.88- 3.95 (m, 1H), 5.05-5.15 (m, 2H), 5.79 (ddt, *J* = 23.8, 10.3, 6.7 Hz, 1H), 5.93 (d, *J* = 0.7 Hz, 1H), 6.23 (dd, *J* = 5.7, 1.1 Hz, 1H), 7.21 (dd, *J* = 5.7, 0.6 Hz, 1H).

^{13}C NMR (125 MHz, $CDCl_3$) δ 33.97, 69.70, 103.38, 117.35, 125.23, 134.20, 150.36, 170.59.

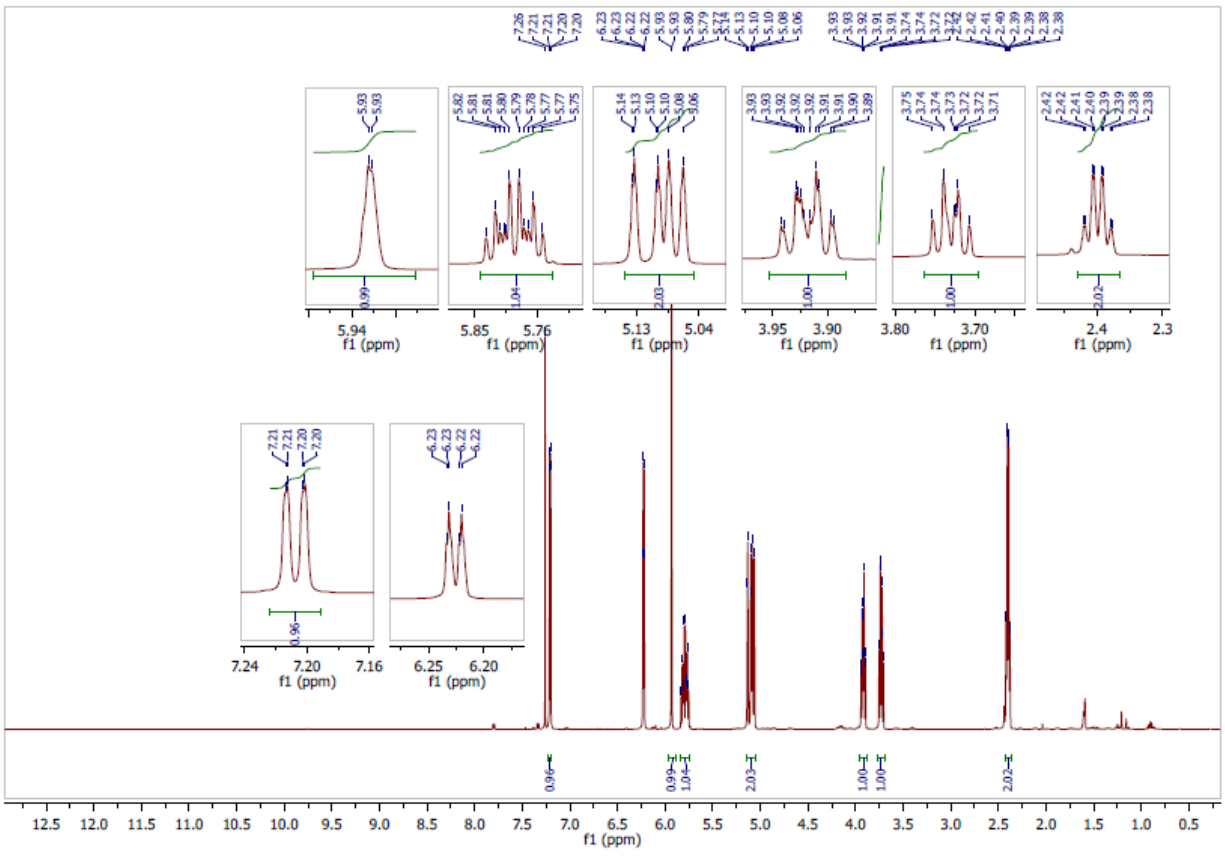

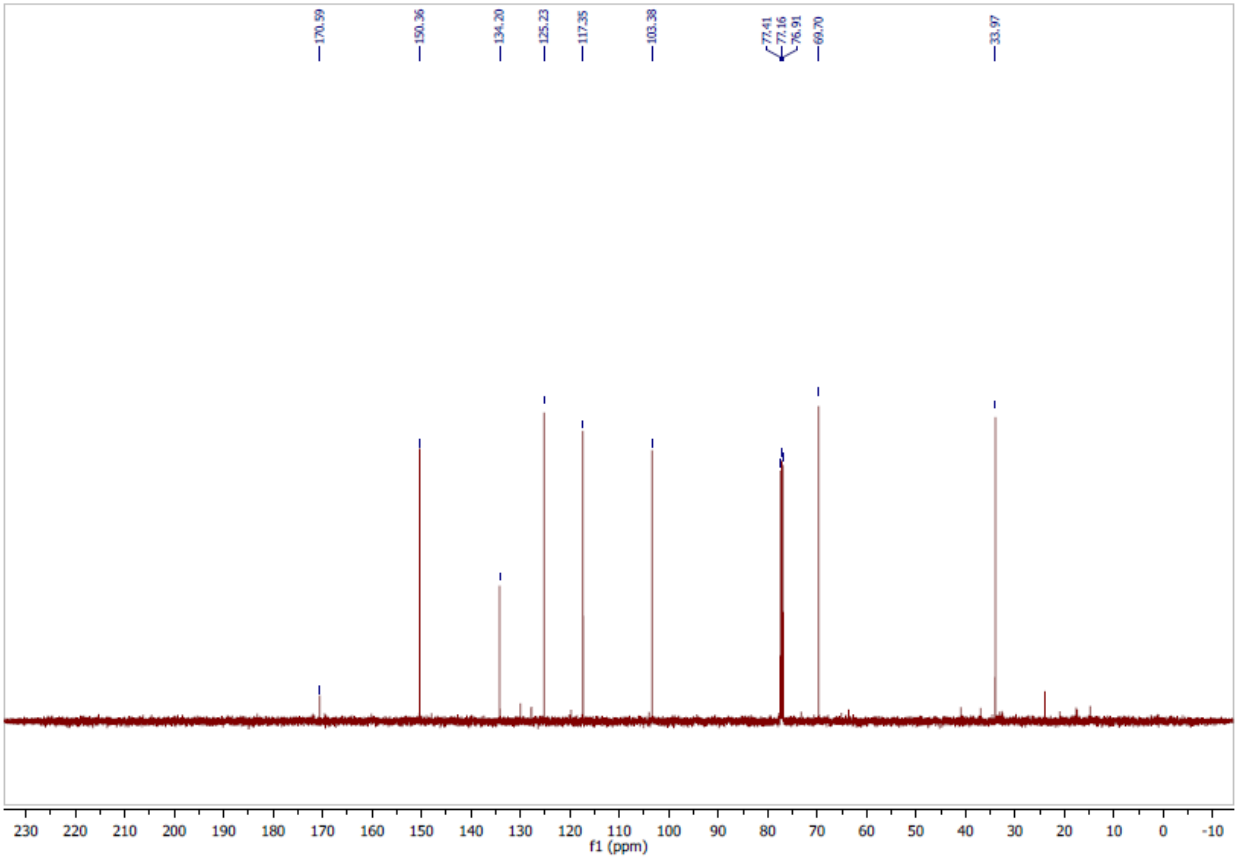

[12] J. G. H. Hermens, T. Freese, K. J. van den Berg, R. van Gemert, B. L. Feringa*, Sci. Adv.*, **2020**, *6*, eabe0026.

Experimental Section

A batch of Elium® 190 thermoplastic resins was generously supplied by Arkema (Lacq, France). Phenyl *bis*(2,4,6-trimethylbenzoyl)phosphine oxide (BAPO) were supplied by Lambson and used as photoinitiating system (PIS). 3 %wt of BAPO was dispersed directly into monomers in a unique cartridge. Then, a Jasco 6600 Real-Time Fourier Transformed Infrared Spectrometer (RT-FTIR) was used to monitor the methacrylate function conversion versus time for the polymerization of samples with 2 mm thickness. Evolution of the near infrared methacrylate C=C double bond peak was followed from 6050 to 6250 cm^{-1} during 600 sec. Rapid Scan was achieved for fast spectral acquisition, using an interval of 1 second. In parallel, photoactivation started after 20 seconds and will be pursued during the whole time of FTIR monitoring by using a LED^{405nm} (Thorlabs) having a light irradiance at the sample of 110 mW/cm^2.

Thermal properties of the different polymers was monitored by DSC. The following sequence was used: first heating with 10°C.min^{-1} rate from -50 to 150°C with 5 min. of isotherm at the two extreme temperatures, then on cooling with the same temperature rate and finally the second heating, with also a heating rate at 10°C/min from -50 to 150°C with 5 min. of isotherm at the two extreme temperatures. The equipment used was a Mettler-Toledo DSC 821e differential scanning calorimeter equipped with a sample robot and Haake EK90/MT intracooler. All DSC curing experiments were performed with a dry nitrogen gas flow of 50 mL min^{-1}. The data evaluation was performed with the STAR e software.

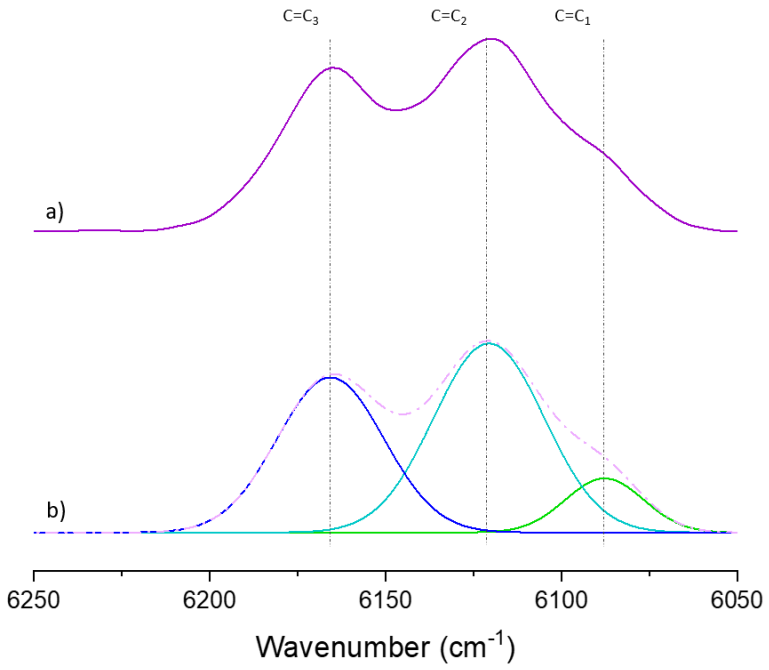

Figure S1: FBI applied to the carbon-carbon stretching band: a) original data (envelope), b) isolated components and cumulative fit peaks.

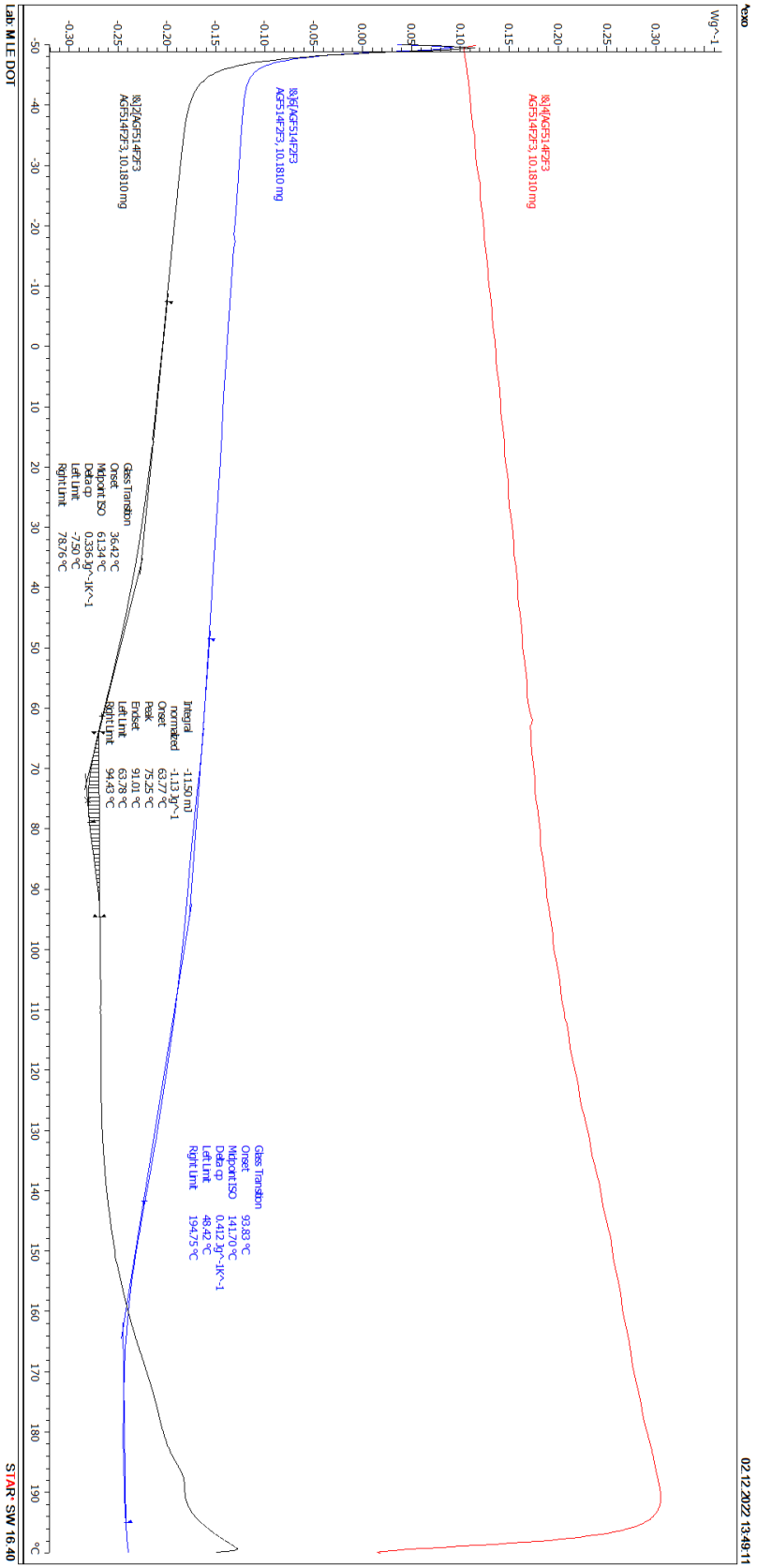

Figure S2: DSC thermogram obtained from the polymer pellet resulting of the homo-polymerization of AF1

Formulations	Peak 1 ($C=C_1$)			Peak 2 ($C=C_2$)			Peak 1 + 2			Peak 3 ($C=C_3$)		
	Conversion (%)	Area (BI^*)	Area (AI^{**})	Conversion (%)	Area (BI^*)	Area (AI^{**})	Conversion (%)	Area (BI^*)	Area (AI^{**})	Conversion (%)	Area (BI^*)	Area (AI^{**})
0 F : 100 E										100	26,87	0
25 F : 75 E	66,0	1,27	0,43	22,0	8,37	6,53	27,8	9,64	6,96	100	19,42	0
50 F : 50 E	70,4	3,99	1,18	-7,3	19,74	21,17	5,8	23,73	22,35	100	15,60	0
75 F : 25 E	59,1	8,14	3,32	-15,4	28,54	32,93	1,2	36,68	36,26	100	8,96	0
100 F : 0 E	47,7	4,98	2,61	56,7	41,33	17,90	55,7	46,31	20,51			

Table S1: RT-FTIR data obtained from Elium® 190 (E) mixed with different weight ratios of 514F2F3 furanone (F) fitted to three C=C double bonds centred at around 6170 cm^{-1} ($C=C_3$), 6120 cm^{-1} ($C=C_2$) and 6080 cm^{-1} ($C=C_1$) before polymerization (BI) and after polymerization (AI**).*

	Peak 1 (C=C$_1$)			Peak 2 (C=C$_1$)			Peak 3 (C=C$_1$)			Peak 4 (C=C$_4$)			Peak 1 + 2 + 3		
	Conversion (%)	Area (BI*)	Area (AI**)	Conversion (%)	Area (BI*)	Area (AI**)	Conversion (%)	Area (BI*)	Area (AI**)	Conversion (%)	Area (BI*)	Area (AI**)	Conversion (%)	Area (BI*)	Area (AI**)
0 F : 100 E										100	11,55	0,00			
25 F : 75 E	100	0,16	0	100	0,77	0,00	100	0,39	0,00	100	8,23	0,00	100	9,55	0
50 F : 50 E				100	1,53	0,00	100	2,56	0,00	100	11,03	0,00	100	15,12	0
75 F : 25 E	100	0,67	0	100	2,58	0,00	100	1,93	0,00	100	9,88	0,00	100	15,06	0
100 F : 0 E	100	0,83	0,08	100	2,53	0,23	96	2,52	0,23	100	7,68	0,00	96	13,56	0,54

Table S2: RT-FTIR data obtained from Elium® 190 (E) mixed with different weight ratios of 533F3 furanone (F) fitted to four C=C double bonds centred at around 6170 cm^{-1} (C=C$_{2\ or/and\ 3}$), 6128 cm^{-1} (C=C$_1$), 6107 cm^{-1} (C=C$_1$) and 6084 cm^{-1} (C=C$_1$) before polymerization (BI) and after polymerization (AI**).* Problème des conversions dans cette table?

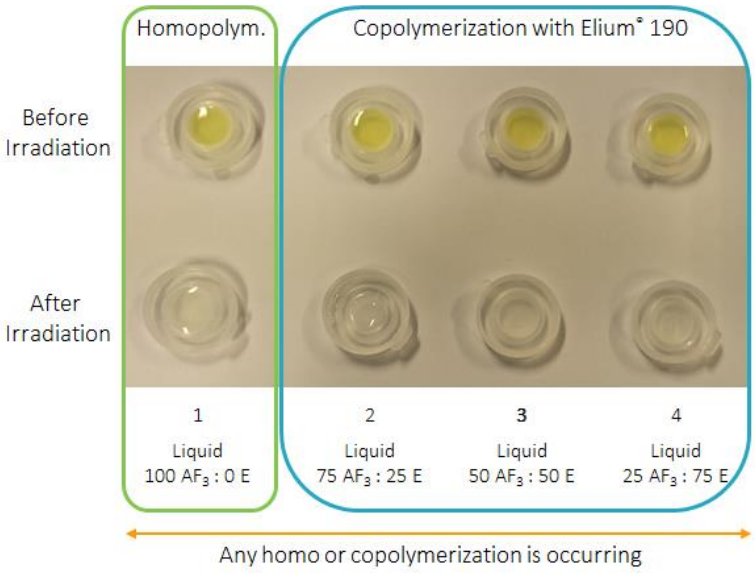

Figure S3: Absence of homo or copolymerizations of AF_3.